Long-Range Lateral Dyke Propagation is Independent of the Level of Neutral Buoyancy

Joseph A. Cartwright[1], and Martino Foschi[1,2]

[1]Department of Earth Sciences, University of Oxford, South Parks Road, Oxford OX1 3AN, UK
[2]Halliburton, 97 Jubilee Ave, Abingdon OX14 4RW, UK

ABSTRACT

Lateral dyke propagation is a fundamental component of magmatic plumbing systems and a key process in crustal construction at mid-ocean ridges and large igneous provinces. Classical models attribute the tendency for lateral magma transport to the Level of Neutral Buoyancy (LNB), where magma density equals host rock density and vertical ascent stalls, forcing lateral propagation. While this concept explains many observations in shallow magmatic systems, its applicability to long-range dyke swarms remains uncertain. The Mull Dyke Swarm (MDS) located in northwest Britain provides a critical test case. Extending over 600 km from its source on Mull, the swarm exhibits a consistently shallow upper tipline, sill emplacement near the surface, and no evidence of eruption along its trajectory. Pressure reconstructions based on associated sill complexes indicate that magma pressures were sufficient to permit eruption over the first 150 km, yet lateral propagation continued. Moreover, calculated LNB depths diverge markedly from observed intrusion geometries. These mismatches suggest that the LNB concept is neither a necessary nor sufficient control on long-range lateral dyke propagation. Instead, propagation is better described as a fracture mechanics problem governed by the competition between magma overpressure, host rock strength, and confining stress. The MDS thus exemplifies a broader class of magmatic systems in which buoyancy plays a minor role in fracture propagation. We argue that lateral dyke emplacement on Earth and other planets should be reframed within the physics of large aspect-ratio hydraulic fractures, rather than buoyancy-driven ascent.

INTRODUCTION

Lateral propagation of dykes is a fundamental aspect of magmatic plumbing systems and is particularly significant for the formation of oceanic crust (Ryan, 1987). This phenomenon has been studied for dyke intrusion events associated with magma reservoirs at shallow depths beneath shield volcanoes in intra-plate settings (Rubin and Pollard, 1987) or at mid ocean ridges (Woods et al., 2019) where the lateral propagation is of the order of 10s of km and aspect ratios of the blade-like dykes is c. 10:1. Long-range lateral propagation exceeding distances of 100s to

1000s of km is, however, widely observed in hundreds of giant radial dyke swarms on Earth, Venus and Mars with aspect ratios of > 50:1, but is less well understood (Ernst et al., 1995). Long-range lateral propagation of dykes requires that they do not break the surface before reaching their ultimate length (Ernst et al., 1995).

Theoretical models accounting for lateral propagation of dykes have typically attributed the lack of surface eruption to buoyancy with a central axis of propagation at the level of neutral buoyancy (LNB) (Lister, 1990) (Fig. 1). The LNB is typically defined at the cross-over in crustal density and magma density where the magma encounters a region of local gravitational equilibrium (local magma density equals local wall rock density) (Walker, 1974; Wilson and Head, 1981; Ryan, 1987). This density contrast is considered to arrest upward propagation and promote lateral propagation (Ryan, 1987; Lister and Kerr, 1991; Fialko and Rubin, 1999). Lateral propagation is thus envisaged to be centered on the LNB precisely because this is the depth where excess magma pressure ΔP (difference between magma pressure and the lithostatic stress) is at its maximum (Fig. 1A) (Ryan, 1987).

Vertically propagating dykes can propagate above the LNB depending on the integrated density profile over the depth range of the magma column (Fig. 1A-B) (Lister and Kerr, 1991; Taisne and Jaupart, 2009). Dykes can overshoot the LNB if they have a deep enough source depth from the dyke initiation position (Wilson and Head, 1981). It is this source depth and magma column height that allows the excess pressure of the magma to remain positive up to the surface and therefore leads to surface eruption (Fig. 1A). Too shallow a source, and there is insufficient buoyant drive gained from denser host rocks to allow the magma to intrude across near surface rocks of lower than magma density (Fig. 1B) (Walker, 1989).

A number of studies have challenged the role of the LNB in magma plumbing in the lithosphere in diverse tectonic settings and magmatic systems. These include the emplacement of granitic magmas (Vigneresse and Clemens, 2000), the intrusion and extrusion of intermediate magmas in arc settings (Loucks, 2014) and the role of volatiles on magma ascent in a range of arc settings (Rasmussen et al., 2022). Most recently, the commonly stated view that the lateral propagation of giant dyke swarms is linked to the LNB has been challenged by a study that modelled the magma pressure distribution in the Mull Dyke Swarm (MDS) in NW Britain (Foschi and Cartwright, 2025).

The aim here is to analyze the MDS and its deviation from theoretically expected behavior to discuss more widely and fundamentally the question of whether the LNB is at all relevant to the physics of long-range lateral dyke propagation. From this, we argue that the physics of fluid pressure driven fractures, such as dykes, is solely a contest between magma pressure and rock strength and that the concept of buoyancy force acting to control propagation only strictly applies to vertically dominated dyke propagation.

THE MULL DYKE SWARM

The MDS was intruded during the later stages of the main period of activity in the British and Irish Igneous Province and is dated at around 58 Ma (Kerr et al., 1999; Chambers and Pringle, 2001). The NW-SE to WNW-ESE trending MDS emanated from a sub-volcanic magma source on the island of Mull (Fig. 2). Geochemical modelling shows that this source consisted of two magma reservoirs, a shallow chamber at c. 7-8 km and a deeper one at or close to the Moho (Morrison et al., 1985; Macdonald et al., 2010, 2015; Ishizuka et al., 2017). Three major sub-swarms of dykes cross major crustal domain boundaries in their > 500 km ESE trajectory to their

terminus in the North Sea, making them amongst the longest continuously mapped dykes on Earth (Fig. 2A) (Carver et al., 2023). Intrusive volumes for these three sub-swarms range from c. 100 to c. 200 km^3, implying an almost complete evacuation of the sub-volcanic reservoir, expressed in the remains of the volcanic superstructure as ring complexes (Carver et al., 2023). A reconstruction of the simplified geology along the strike of the MDS shows that the dykes transected major crustal domains with contrasting crustal density profiles (Fig. 2B), from crystalline dominated rocks to thick sedimentary basin fills with lower densities than the typical range of basaltic magma densities. Critically, the upper tips of the dykes approached to within a kilometer or less of the contemporaneous surface along the entire strike length with no evidence of surface eruption of basaltic magma. Had there been eruption *en-route*, the dykes would almost certainly have terminated close to the eruption site (Ernst et al., 1995).

At least five separate dyke-fed sills or sill complexes were emplaced at shallow crustal levels along the trajectory of the sub-swarms during dyke propagation (Foschi and Cartwright, 2025). They used these sills as piezometers to reconstruct the minimum magma pressure required for their formation and extrapolated upwards to find the excess magma pressure at surface (P_0). They found that P_0 was positive for the first 150 km of the dyke trajectory implying that surface eruption should have occurred on purely buoyancy grounds (Fig. 2C). Using known crustal density values, they computed the depth range for the LNB along the path followed by the main sub-swarms. They found that the LNB was at the surface close to Mull and plunged to ~8 km at the distal limits of the swarm (Fig. 2B).

Here, we were motivated to explore the probable range of upper arrest depths (tipline) if propagation was driven by buoyancy using the concept of the LNB as a basis for the analysis. Using a realistic range of magma and crustal densities and a maximum reservoir depth of 10 km

(Ishizuka et al., 2017), we computed the range of depths at which dykes would arrest upwards if the vertical component of dyke propagation was driven by buoyancy (see Supplementary Information). Importantly, this Monte Carlo simulation showed that these arrest depths are consistently several kilometers deeper than the inferred depths of the upper tips derived from seismic interpretation and aeromagnetic modelling, validated by direct well calibration (Carver et al., 2023; Pryce et al., 2025; Cartwright et al. 2025, their Fig. 9) (Fig. 2D).

DISCUSSION

Three main arguments can be advanced from the evidence provided by the MDS that lateral propagation is not dependent on the LNB. Firstly, the geometry of the upper tip of the main dykes does not follow the reconstructed depth for the LNB along the dyke transect. If lateral propagation was centered at the LNB as represented in earlier models (e.g., Ryan, 1987; Fialko and Rubin, 1999), the dyke center line would plunge by up to 8 km over the strike length of the major dykes (Fig. 2B). This seems highly unlikely given the contradicting geological evidence showing an almost horizontal upper tipline (Foschi and Cartwright, 2025) (Fig. 2B).

Secondly, if magma ascent was purely by buoyancy in this area, then based on the LNB position and a full range of magma densities, the dykes would have stalled at depths > ~3–5.6 km below the observed dyke-fed sill complexes in the distal parts of the MDS (Fig. 2D). These sills provide very good estimates of the minimum magma pressure and indicate upper tip positions 6–8 km above the LNB and 2.5–4.5 km above the predicted buoyancy-driven arrest depth.

Thirdly, proximal to the Mull magma reservoir, the LNB lies above the ground surface for nearly 50 km. If dykes were driven by buoyancy they should have breached the surface and magma would have erupted. Given that the major dykes failed to erupt and continued to propagate over

500 km laterally to the southeast, it is evident that the LNB did not control the propagation geometry.

These arguments demonstrate that the LNB exerted little to no control on dyke emplacement of the MDS. Instead, we argue that dyke geometry reflects the interplay between magma pressure, host-rock strength, and confining stress. This interplay of stresses and pressures is instead consistent with the mechanical frameworks of Rubin (1995) and Buck et al. (2004). As Rubin (1995) emphasized, "magma within a dyke senses the density of the host rock only insofar as that density contributes to the ambient stress normal to the dyke plane." Therefore, for lateral propagation, the critical parameters are magma pressure distribution and stress heterogeneity, not buoyancy relative to crustal density structure.

The difference in the potential for the LNB to influence a dominantly vertically propagating dyke as opposed to one that is dominantly laterally propagating is illustrated with a conceptual figure (Fig. 3A-B). In the vertical case (Fig. 3A-B, location X_0), dyke initiation above a sill-like chamber requires magma pressure (P_M) to exceed the total vertical stress (σ_V). Following Rubin and Pollard (1987), a lower bound for the reservoir magma pressure required for failure of the overlying rock units is equal to the total vertical stress of the rocks capping the reservoir, σ_V. Here, buoyancy and rock-column density govern whether the dyke can reach the surface and result into a subaerial eruption of magma and a formation of a volcanic edifice (Fig. 3A-B, X_0). This model requires also that the LNB is positioned at a depth that allows an excess pressure at the surface to be greater than zero. Conversely, far away from the volcanic source the pressure at X_1 is independent of the density structure of the rock column above the source even if the actual density structure has changed over distance. The only condition necessary to sustain lateral dyke

147 propagation is that magma pressure exceeds the minimum horizontal stress, a fraction of the total
148 vertical stress.
149 In a dominantly laterally propagating dyke, nucleation occurs at the margins of a sill-like magma
150 chamber where tensile stress concentrates during sill inflation (Gudmundsson, 2020). The
151 injection pressure (P_{inj}) at the chamber margin is related to the vertical confining stress there,
152 but once the dyke propagates away from the reservoir, the magma pressure at a given depth is
153 determined by P_{inj} minus lateral pressure losses due to viscous flow and fracture propagation
154 (Macdonald et al., 1988; Lister and Kerr, 1991). Consequently, the pressure distribution in a
155 lateral dyke becomes largely independent of the local overburden density and of the LNB; the
156 vertical magma gradient is then controlled by magma density, height above the injection point
157 (e.g., the depth of the sill-like magma chamber), viscous losses, and work done in propagation
158 against the minimum horizontal stress, σ_{Hmin}.
159 This conceptual model for lateral dyke pressure distributions can be extended to giant radial dyke
160 swarms on other terrestrial planets (Ernst et al., 1995). Although reservoir dimensions are poorly
161 known, their diameters are typically small compared to the lateral lengths of the dykes that they
162 feed (c.f., Wilson and Head, 1992).
163 To reinforce how challenging it would be to explain long-range lateral propagation with a
164 dominantly buoyant driver, we directly contrast these two propagation mechanisms. In the case
165 of a buoyancy-driven dyke, vertical ascent stalls at the LNB and the dyke then spreads laterally.
166 This process requires large density contrasts and buoyancy forces to drive magma hundreds or
167 thousands of kilometers laterally (Lister and Kerr, 1991). This propagation geometry with an
168 inverted tear drop shape (buoyant plume) is physically analogous to CO_2 ascending in a water

saturated reservoir and spreading laterally beneath a regional seal (e.g., Huppert and Woods, 1995).

In the case of a dominantly laterally propagating dyke, lateral propagation initiates at the reservoir margin (similar to that shown in Fig. 3A) and is governed from the outset by the injection pressure and sustained magma supply. The lateral variations in density only affect resistance to fracture, not the driving pressure.

In summary, there is no doubt that buoyancy influences magma plumbing where magma ascends dominantly vertically. As elegantly argued by Ryan (1987) and Walker (1989) this accounts for observations of both inactive and active magmatic plumbing systems. However, the concept of the LNB does not explain our observations of long-range lateral propagation of the MDS.

We argue that magmatic plumbing systems cannot all be viewed in the conceptual framework of buoyant magma ascent. The sources of magma pressure are undoubtedly dominated by vertical loading onto confined magma source regions, but long-range lateral dyke propagation should not be analyzed as a buoyancy-driven process. Similar reservations undoubtedly apply to many other types of intrusive and extrusive magmatism and warrant a renewed research effort directed at identifying the contributory factors governing magma pressure distributions.

ACKNOWLEDGMENTS

We are grateful to SLB for provision of an academic license of Petrel. The paper contains information provided by the Oil and Gas Authority and/or other third parties.

REFERENCES CITED (29)

Buck, W.R., Einarsson, P. and Brandsdóttir, B., 2006. Tectonic stress and magma chamber size as controls on dike propagation: Constraints from the 1975–1984 Krafla rifting episode. Journal of Geophysical Research: Solid Earth, 111(B12). https://doi.org/10.1029/2005JB003879

Cartwright, J., Foschi, M. and Phillips, D., 2025. The role of sill intrusion in delimiting the lateral propagation of giant dyke swarms: emplacement of the Dogger Sill Complex, southern North Sea. Journal of the Geological Society, pp.jgs2025-005. https://doi.org/10.1144/jgs2025-005

Carver, F., Cartwright, J., McGrandle, A., Kirkham, C. and Pryce, E., 2023. The continuation of the Mull Dyke Swarm into the Southern North Sea. Journal of the Geological Society, 180(6), pp.jgs2023-039. https://doi.org/10.1144/jgs2023-039

Chambers, L.M. and Pringle, M.S., 2001. Age and duration of activity at the Isle of Mull Tertiary igneous centre, Scotland, and confirmation of the existence of subchrons during Anomaly 26r. Earth and Planetary Science Letters, 193, 333-345. https://doi.org/10.1016/S0012-821X(01)00499-X

Ernst, R.E., Head, J.W., Parfitt, E., Grosfils, E. and Wilson, L., 1995. Giant radiating dyke swarms on Earth and Venus. Earth-Science Reviews, 39, 1-58. https://doi.org/10.1016/0012-8252(95)00017-5

Fialko, Y.A. and Rubin, A.M. 1999. Thermal and mechanical aspects of magma emplacement in giant dyke swarms. Journal of Geophysical Research, 104 (B10), 23,033 -23,049. https://doi.org/10.1029/1999JB900213

Foschi, M. and Cartwright, J.A., 2025. Constraints on magma pressure distribution during long range lateral propagation of giant radial dyke swarms. Journal of Geophysical Research: Solid Earth, 130(10), 2025JB031995. https://doi.org/10.1029/2025JB031995

Gudmundsson, A., 2020. Volcanotectonics: Understanding the structure, deformation and dynamics of volcanoes. Cambridge University Press. https://doi.org/10.1017/9781139176217

Huppert, H.E. and Woods, A.W., 1995. Gravity-driven flows in porous layers. Journal of Fluid Mechanics, 292, pp.55-69.

Ishizuka, O., Taylor, R.N., Geshi, N. and Mochizuki, N., 2017. Large-volume lateral magma transport from the Mull volcano: An insight to magma chamber processes. Geochemistry, Geophysics, Geosystems, 18, 1618-1640. https://doi.org/10.1002/2016GC006712

Kerr, A.C., Kent, R.W., Thomson, B.A., Seedhouse, J.K. and Donaldson, C.H., 1999. Geochemical evolution of the Tertiary Mull volcano, western Scotland. Journal of Petrology, 40, 873-908. https://doi.org/10.1093/petroj/40.6.873

Lister, J.R., 1990. Buoyancy-driven fluid fracture: similarity solutions for the horizontal and vertical propagation of fluid-filled cracks. Journal of Fluid Mechanics, 217, pp.213-239. https://doi.org/10.1017/S0022112090000696

Lister, J.R. and Kerr, R.C., 1991. Fluid-mechanical models of crack propagation and their application to magma transport in dykes. Journal of Geophysical Research: Solid Earth, 96(B6), https://doi.org/10.1029/91JB00600

Loucks, R.R., 2014. Distinctive composition of copper-ore-forming arc magmas. Australian Journal of Earth Sciences, 61(1), pp.5-16.

Macdonald, R., Wilson, L., Thorpe, R.S. and Martin, A., 1988. Emplacement of the Cleveland dyke: evidence from geochemistry, mineralogy, and physical modelling. Journal of Petrology, 29, 559-583. https://doi.org/10.1093/petrology/29.3.559

Macdonald, R., Baginski, B., Upton, B.G.J., Pinkerton, H., MacInnes, D.A. and MacGillivray, J.C., 2010. The Mull Palaeogene dyke swarm: Insights into the evolution of the Mull igneous centre and dyke-emplacement mechanisms. Mineralogical Magazine, 74(4), pp.601-622. https://doi.org/10.1180/minmag.2010.074.4.601

Macdonald, R., Fettes, D.J. and Bagiński, B., 2015. The Mull Paleocene dykes: some insights into the nature of major dyke swarms. Scottish Journal of Geology, 51(2), pp.116-124. https://doi.org/10.1144/sjg2014-016

Morrison, M.A., Thompson, R.N. and Dickin, A.P., 1985. Geochemical evidence for complex magmatic plumbing during development of a continental volcanic center. Geology, 13(8), pp.581-584. https://doi.org/10.1130/0091-7613(1985)13<581:GEFCMP>2.0.CO;2

Pryce, E., Cartwright, J., Kirkham, C. and Phillips, D., 2025. Sequential phreatomagmatic eruptions during the lateral propagation of giant dyke swarms. Geology, 53(3), pp.274-278. https://doi.org/10.1130/G52490.1

Rasmussen, D.J., Plank, T.A., Roman, D.C. and Zimmer, M.M., 2022. Magmatic water content controls the pre-eruptive depth of arc magmas. *Science*, *375*(6585), pp.1169-1172. DOI: 10.1126/science.abm5174

Rubin, A.M. and Pollard, D.D., 1987. Origins of blade-like dikes in volcanic rift zones. US Geological Survey Professional Paper, 1350(2), pp.1449-1470.

255 Rubin, A.M., 1995. Propagation of magma-filled cracks. Annual Review of Earth and Planetary
256 Sciences, Volume 23, pp. 287-336., 23, pp.287-336.
257 https://doi.org/10.1146/annurev.ea.23.050195.001443
258 Ryan, M.P. 1987. Neutral buoyancy and the mechanical evolution of magmatic systems. (Ed.),
259 Magmatic Processes: Physico-chemical Principles, edited by B.O. Mysen pp 259-187,
260 The Geochemical Society, University Park, Pa.
261 Taisne, B., and Jaupart, C. 2009. Dike propagation through layered rocks. Journal of
262 Geophysical Research, 114, B09203. https://doi.org/10.1029/2008JB006228
263 Vigneresse, J.A. and Clemens, J.D., 2000. Granitic magma ascent and emplacement: neither
264 diapirism nor neutral buoyancy. Geological Society, London, Special Publications,
265 174(1), pp.1-19.
266 Walker, G.P., 1974. The structure of eastern Iceland. In Geodynamics of Iceland and the North
267 Atlantic Area: Proceedings of the NATO Advanced Study Institute held in Reykjavik,
268 Iceland, 1–7 July, 1974 (pp. 177-188). Dordrecht: Springer Netherlands.
269 Walker, G.P., 1989. Gravitational (density) controls on volcanism, magma chambers and
270 intrusions. Australian Journal of Earth Sciences, 36(2), pp.149-165.
271 https://doi.org/10.1080/08120098908729479
272 Wilson, L. and Head III, J.W., 1981. Ascent and eruption of basaltic magma on the Earth and
273 Moon. Journal of Geophysical Research: Solid Earth, 86(B4), pp.2971-3001.
274 https://doi.org/10.1029/JB086iB04p02971
275 Woods, J., Winder, T., White, R.S. and Brandsdóttir, B., 2019. Evolution of a lateral dike
276 intrusion revealed by relatively-relocated dike-induced earthquakes: The 2014–15

Bárðarbunga–Holuhraun rifting event, Iceland. Earth and Planetary Science Letters, 506, pp.53-63. https://doi.org/10.1016/j.epsl.2018.10.032

FIGURE CAPTIONS

Figure 1. Definition of the Level of Neutral Buoyancy (LNB) as a function of depth. A: a dyke sourced within the mantle (here at 50 km below the surface) has enough excess pressure to overshoot the LNB and erupt magma at surface (modified from Lister and Kerr, 1991). B: a dyke sourced at a shallow magma reservoir (here at 15 km below the surface) is unable to reach the surface.

Figure 2. A: Simplified outline map of the Mull Dyke Swarm from the onshore and offshore areas over which it extends. Onshore dyke traces are from the British Geological Survey 1:250,000 sheets of N. England and S. Scotland; offshore dyke traces are from Carver et al., 2023). B: Simplified geology along the approximate mid-position of the MDS in its transect from Mull to the southern North Sea (modified after Foschi and Cartwright, 2025) with dyke outline, Level of Neutral Buoyancy (LNB) boxplots at known sill locations, and indicative continuous depth of the LNB depth over the distance of the dyke. C: Excess magma pressure at surface P_0 at six locations referenced to distance from Mull. The first 3 locations from Mull are consistent with subaerial eruption (inconsistent with observations, see text). D: Depth of dyke tip line relative to distance from Mull based on buoyancy only (see Supplementary Information).

Figure 3. A: Schematic profile of two dykes emanating from a sill-like magma chamber (source) from its crest and its lateral margin, with indicative time evolution contours of the dyke body, depth of the Level of Neutral Buoyancy (LNB), and host rock consistent with increasing density structure with depth (not to scale). The dyke from the crest results into an eruption and the formation of a volcanic edifice. The dyke from the lateral margin of the chamber results into a laterally propagating dyke without eruption. B: Pressure and depth plots and schematic profiles for location X_0 and X_1. At X_0 the magma pressure P_M is larger than the σ_V and results in an eruption. At X_1 the magma pressure P_M is larger than the σ_{Hmin} and results in an advancement of the dyke laterally (into the page). The dyke does not erupt because the pressure is equal to the σ_{Hmin} at its tipline.

310

Figure 1

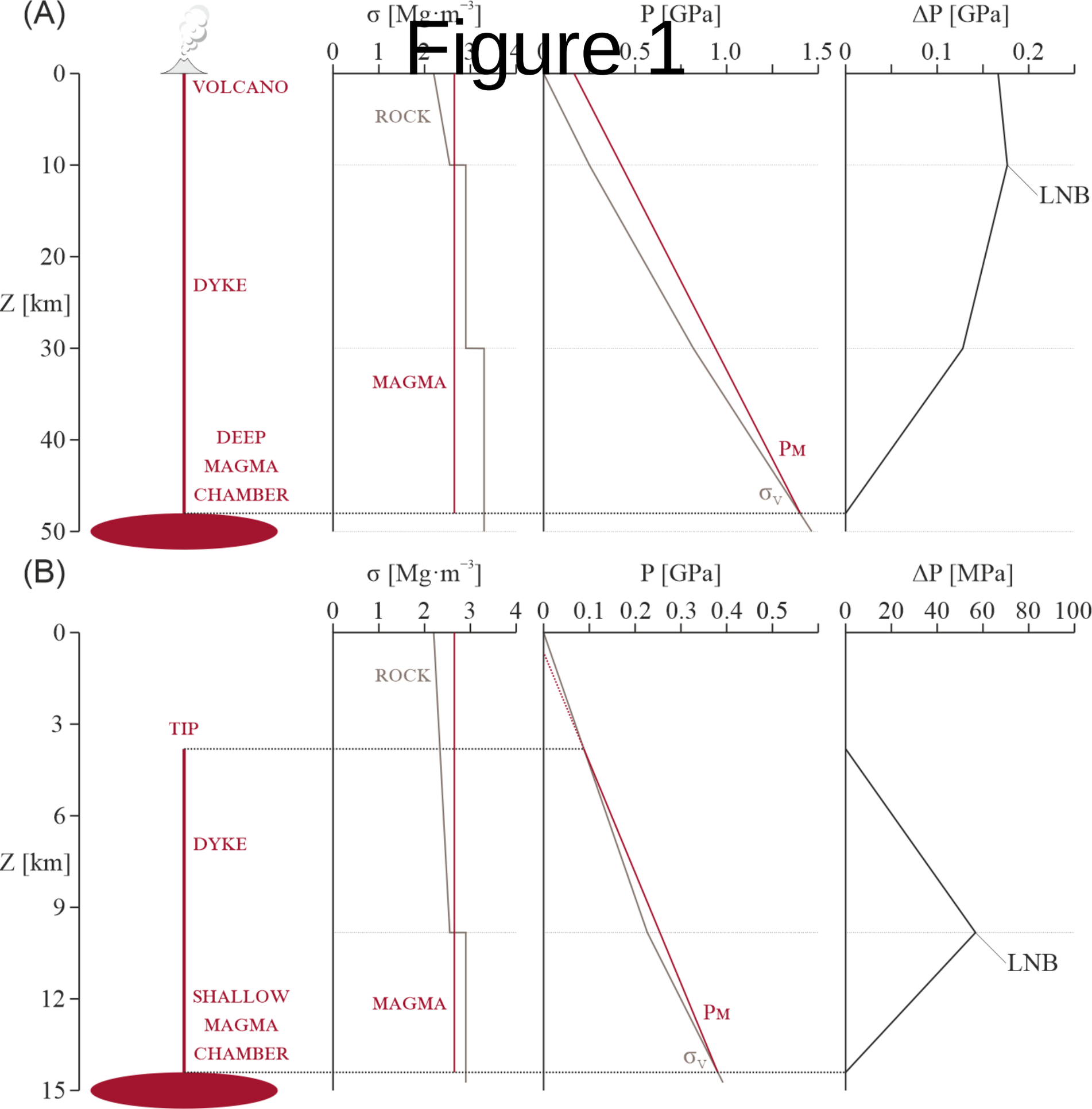
(A)
σ [Mg·m⁻³]
P [GPa]
ΔP [GPa]
VOLCANO
ROCK
DYKE
MAGMA
DEEP
MAGMA
CHAMBER
LNB
PM
σV
Z [km]
(B)
σ [Mg·m⁻³]
P [GPa]
ΔP [MPa]
ROCK
TIP
DYKE
SHALLOW
MAGMA
CHAMBER
MAGMA
LNB
PM
σV
Z [km]

Figure 2

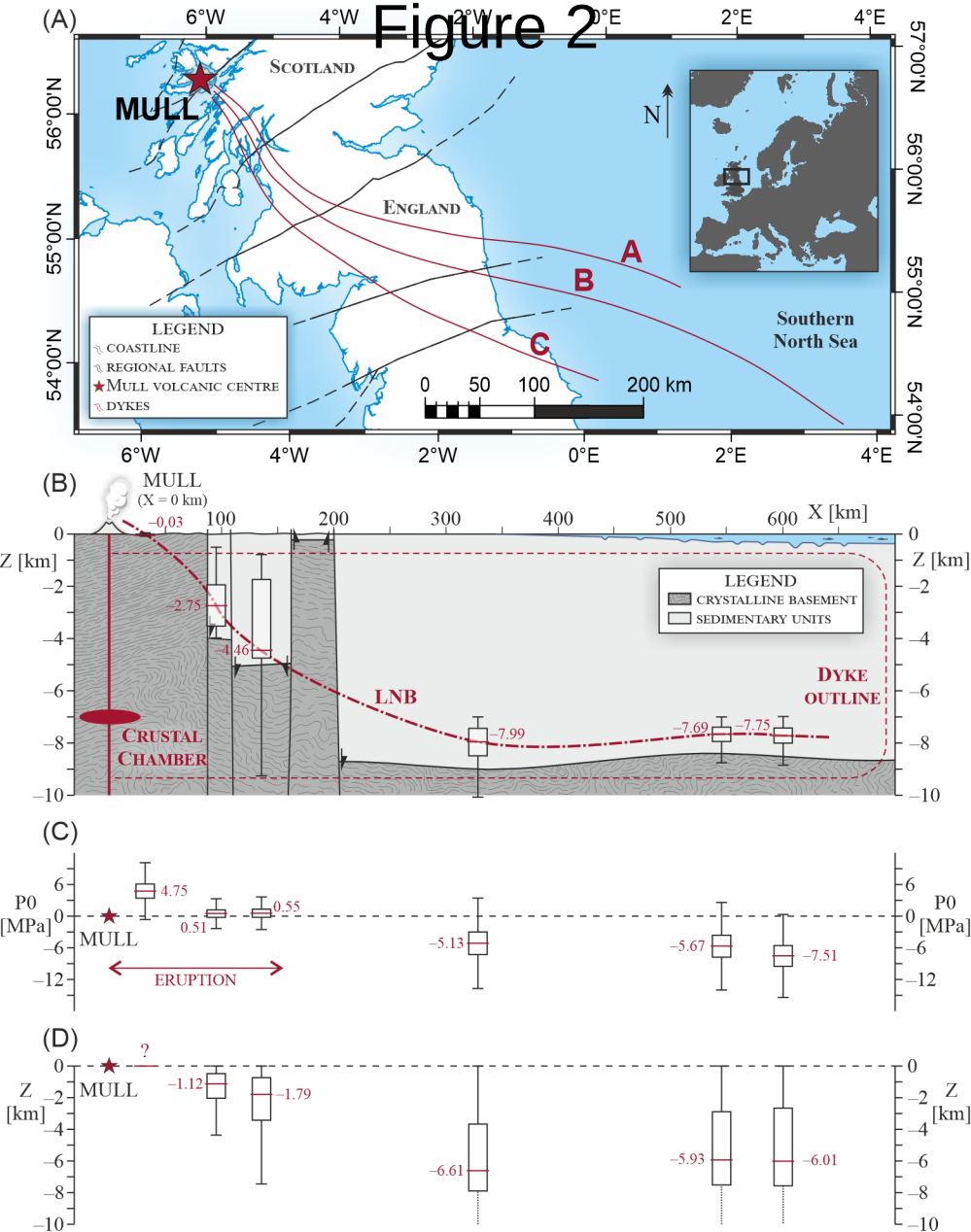
(A)
6°W
4°W
2°W
0°E
2°E
4°E
57°00'N
56°00'N
55°00'N
54°00'N
SCOTLAND
MULL
ENGLAND
N
A
B
C
Southern
North Sea
LEGEND
COASTLINE
REGIONAL FAULTS
MULL VOLCANIC CENTRE
DYKES
0 50 100 200 km
(B)
MULL
(X = 0 km)
X [km]
Z [km]
LEGEND
CRYSTALLINE BASEMENT
SEDIMENTARY UNITS
DYKE
OUTLINE
LNB
CRUSTAL
CHAMBER
−0,03
−2.75
−4.46
−7.99
−7.69
−7.75
(C)
P0
[MPa]
MULL
ERUPTION
4.75
0.51
0.55
−5.13
−5.67
−7.51
(D)
Z
[km]
MULL
?
−1.12
−1.79
−6.61
−5.93
−6.01

Figure 3

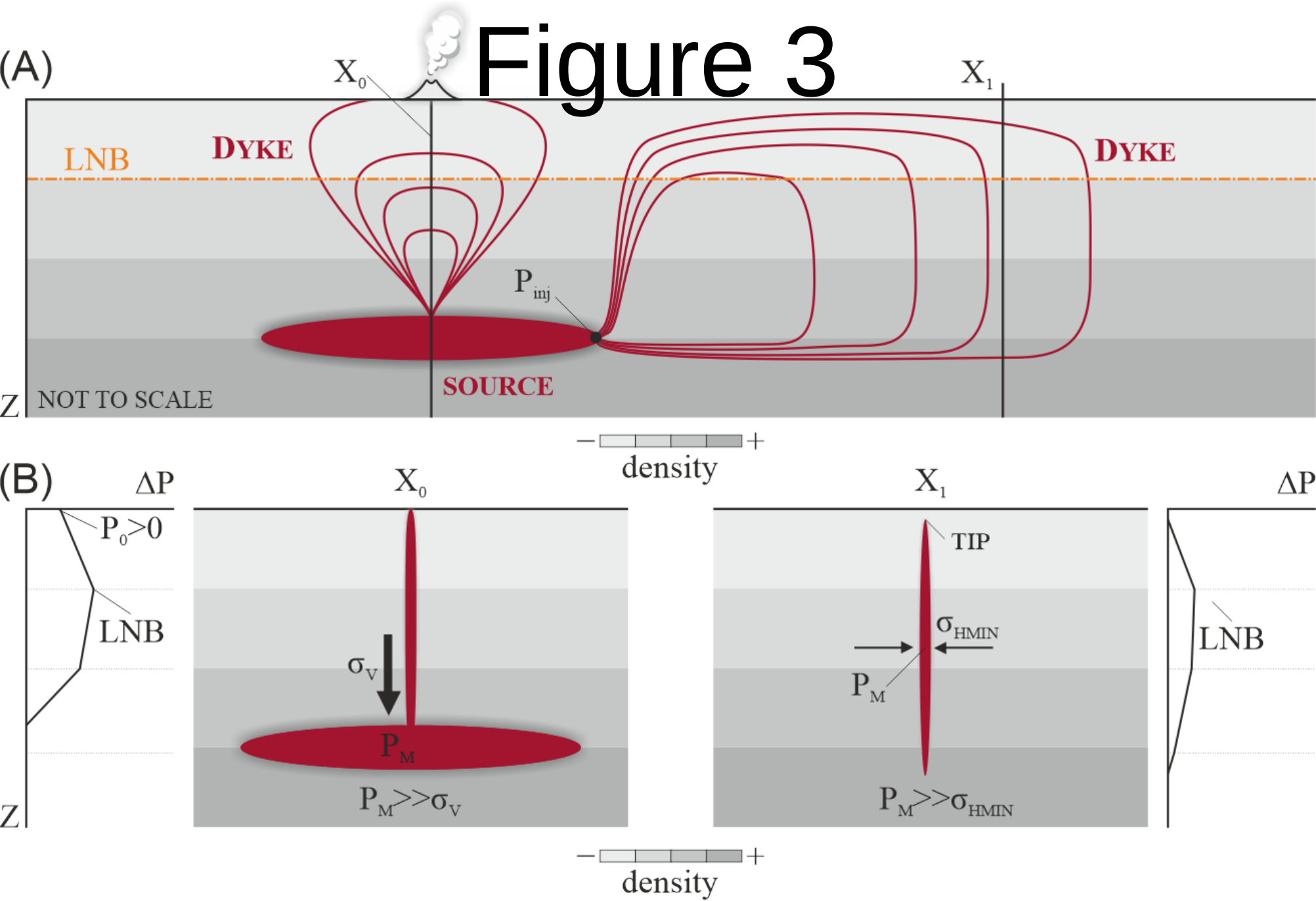
(A)
X0
X1
LNB
DYKE
DYKE
Pinj
SOURCE
Z
NOT TO SCALE
density
(B)
ΔP
X0
X1
ΔP
P0>0
LNB
TIP
σV
σHMIN
PM
PM
PM>>σV
PM>>σHMIN
LNB
Z
density